**Supplemental Figures**

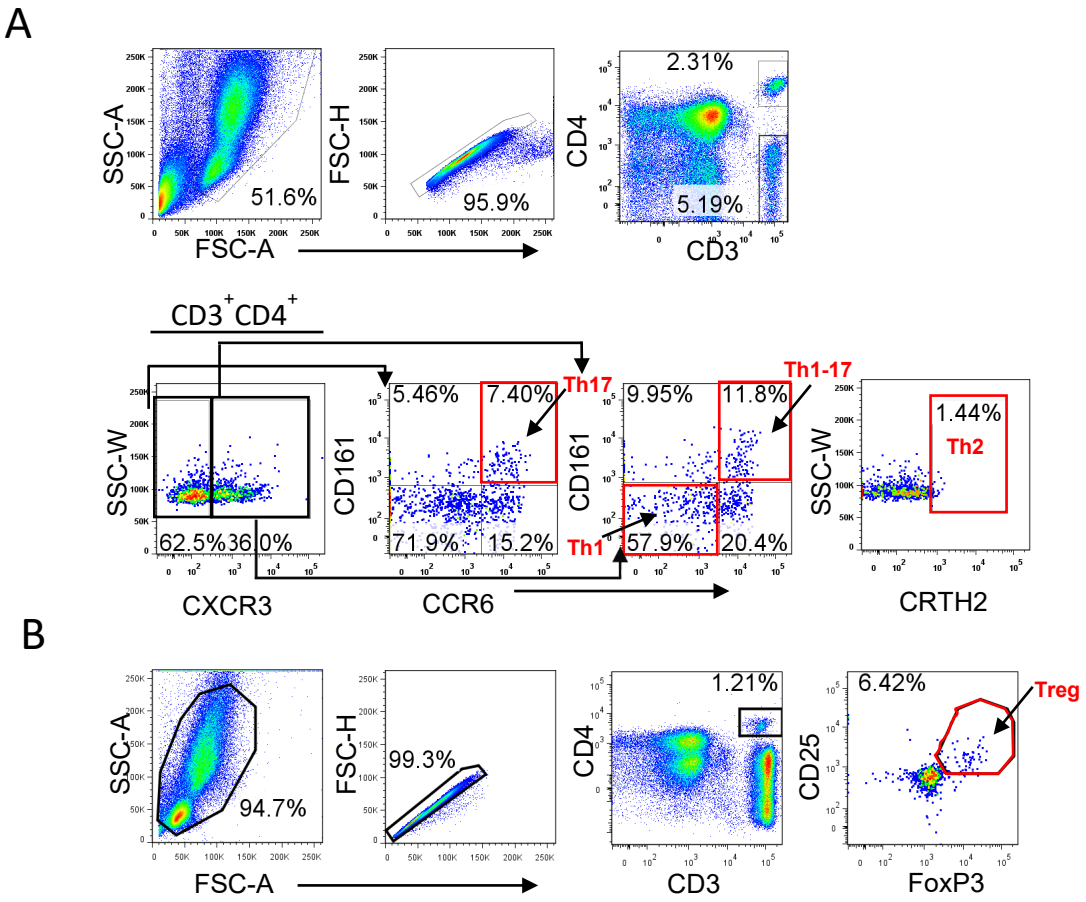


**Supplemental Figure 1. Example of Gating Strategy for Th1, Th17, Th1-Th17, Th2 and Treg.** (A) Th1, Th17, Th1-Th17 and Th2 Gating. PBMCs isolated using a Ficoll-hypaque density gradient centrifugation were stained with fluorochrome-conjugated anti-CD3, CD4, CXCR3, CD161, CCR6 and CRTH2. The stained cells were then analyzed using the BD FACSCanto™ II system followed by data analysis using Flowjo 7.6.5. T helper subsets are marked and defined as follows: Th1: $CD3^+CD4^+CXCR3^+CCR6^-CD161^-$; Th17: $CD3^+CD4^+CXCR3^-CCR6^+CD161^+$; Th1-Th17: $CD3^+CD4^+CXCR3^+CCR6^+CD161^+$; Th2: $CD3^+CD4^+CXCR3^-CCR6^-CD161^-CRTH2$ ($CD294^+$). SSC-A/W: Side Scatter Area/Width, FSC-A/H: Forward Scatter Area/Height. (B) Treg Gating. PBMCs were stained with fluorochrome-conjugated anti-CD3, CD4, CD25, followed by fixation and permeabilization using eBioscience™ Foxp3 / Transcription Factor Staining Buffer Set, and stained with flurochorme-conjugated anti-human Fox P3. The stained cells were then

analyzed using the BD FACSCanto™ II system followed by data analysis using Flowjo 7.6.5. Treg are marked and defined as $CD3^{+}CD4^{+}CD25^{+}FoxP3^{+}$

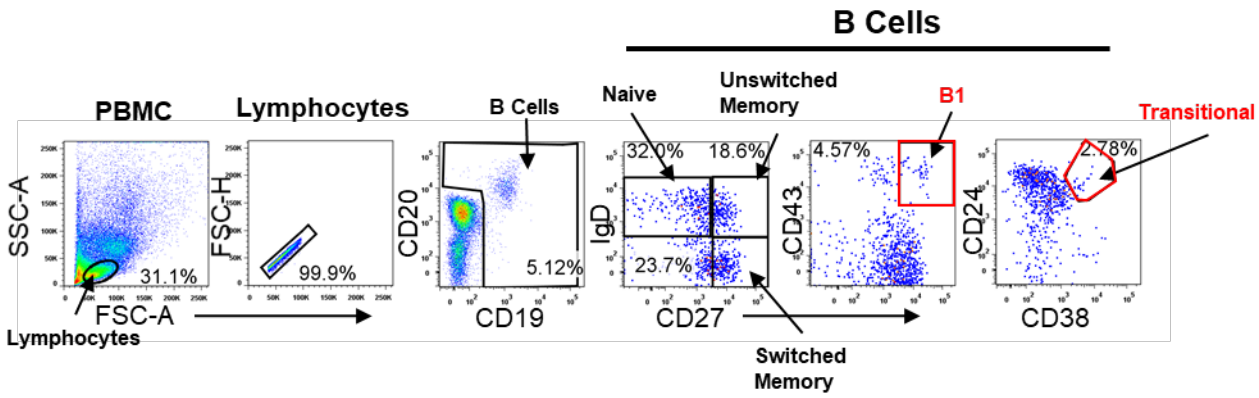


**Supplemental Figure 2. Example of Gating Strategy for B cell subsets.** PBMCs isolated using a Ficoll-hypaque density gradient centrifugation were stained with fluorochrome-conjugated anti-CD19, CD20, CD27, IgD, CD38, CD24 and CD43. The stained cells were then analyzed using the BD FACSCanto™ II system followed by data analysis using Flowjo 7.6.5. B subsets are marked and defined as the following: Memory T cells: $CD20^{+}19^{+}CD27^{+}$; Naive: $CD20^{+}19^{+}CD27^{-}$ $IgD^{+}$; Unswitched Memory B cells: $CD20^{+}19^{+}CD27^{+}$ $IgD^{+}$; Switched Memory B cells: $CD20^{+}19^{+}CD27^{+}$ $IgD^{-}$; Transitional B cells: $CD20^{+}19^{+}CD38^{hi}CD24^{hi}$; B1 cells: $CD20^{+}CD19^{+}CD27^{+}CD43^{+}$.

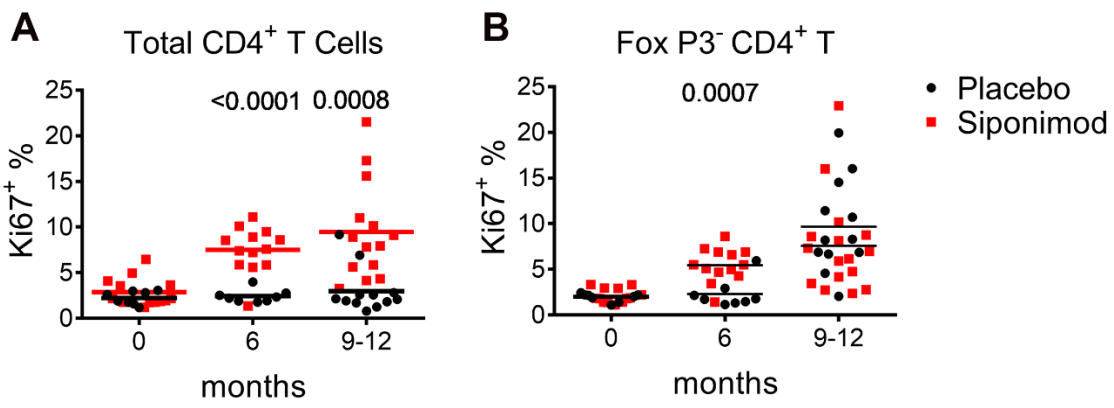


**Supplemental Figure 3 Increased frequency of proliferative CD4$^+$ T cells after siponimod treatment. (A)** Cross-section comparison of Ki67$^+$% of CD4 T at baseline, 6 month and 9-12 month after treatment with placebo or siponimod. (B) Cross-section comparison of Ki67$^+$% of FoxP3$^-$ CD4$^+$ T cells at baseline, 6 month and 9-12 month after treatment with placebo or siponimod. *P* values represent statistically significant different P value between placebo and siponimod at the same time point using Mann-Whitney U test for (A-B) 6 months and 9-12 months; unpaired t test for (B) 0 month; unpaired t test with Welch's correction for (A) 0 month. Placebo (0 month: N=8; 6 months: N=8; 9-12 months: N=12) or Siponimod (0 month: N=13; 6 months: N=13; 9-12 months: N=16).

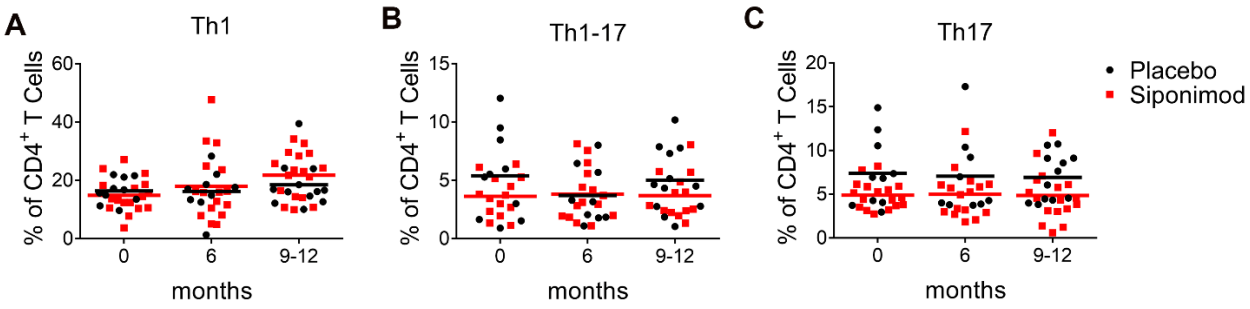


**Supplemental Figure 4**. **Siponimod did not alter the relative frequencies of Th1, Th1-17 and Th17.** Frequencies of effector T cell subsets shown as a fraction of total $CD3^{+}CD4^{+}$ T cells. (A) T helper (Th1) ($CD4^{+}$ $CXCR3^{+}CCR6^{-}CD161^{-}$. (B) Th1-Th17 ($CD4^{+}CXCR3^{+}CCR6^{+}CD161^{+}$). (C) Th17 ($CD4^{+}CXCR3^{-}CCR6^{+}CD161^{+}$). Comparisons were done with multiple t tests with Holm-Sidak adjusted P value. None showed significance. Points represent individual participants, lines show means for placebo (black) and siponimod (red). Placebo N: 0 month=10, 6 months=9, 9-12 months=12; Siponimod N: 0 month=17, 6 months=16, 9-12 months=18.

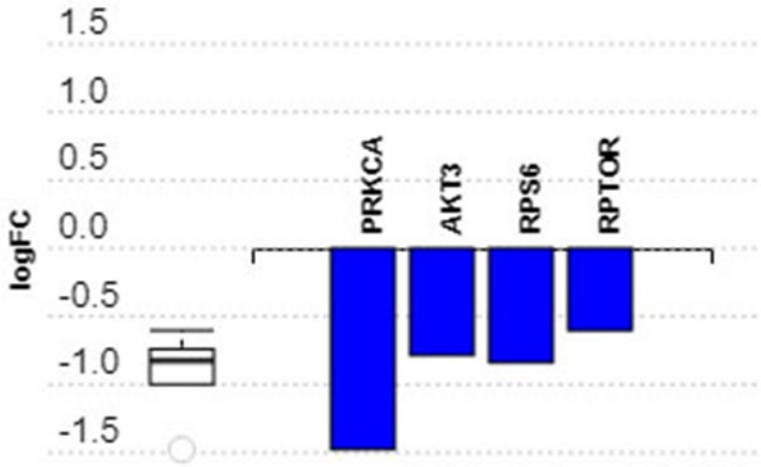


**Supplemental Figure 5. Siponimod alters immune cell gene expression profile leading to downregulation of mTOR pathway.** mRNA content from peripheral blood measured using the Affymetrix Human Gene ST 2.1 microarray from same cohort of patients as in Figures 2 and 3: SPMS patients at baseline (n=21) and after siponimod treatment (n=12) or placebo (n=7). Genes involved in the mTOR signaling pathway decreased following siponimod treatment relative to baseline. The box and whisker plot on the lower left summarizes the distribution of all the differentially expressed genes that are annotated to this GO term. The box represents the 1$^{st}$ quartile, the median, and the 3$^{rd}$ quartile, while the outliers are represented by circles.

# Table 1 Antibodies used in this study

| Vender | Catalog # | Conjugated Antibodies | Clone |
|---|---|---|---|
| **Tonbo Biosciences** | 60-0038-T100 | CD3 PE-Cy7 | UCHT1 |
| **(San Diego, CA.** | 50-0048-T100 | CD4 PE | OKT4 |
| **USA)** | 20-0086-T100 | CD8 APC | OKT8 |
| | 60-0199-T100 | CD19 PE-Cy7 | HIB19 |
| **Biolegend** | 304128 | CD45RA APC-Cy7 | H100 |
| **(San Diego, CA** | 304216 | CD45RO Pacific Blue | UCHL1 |
| **USA)** | 353214 | CCR7 APC | G043H7 |
| | 353716 | CXCR3 Brilliant Violet 421™ | G025H7 |
| | 339936 | CD161-FITC | HP-3G10 |
| | 353406 | CCR6 Per CP-Cy5.5 | G034E3 |
| | 302616 | CD25 Alexa Fluor® 488 | BC96 |
| | 318328 | CD56 Brilliant Violet 421™ | HCD56 |
| | 310936 | CD69 Brilliant Violet 510™ | FN50 |
| | 317444 | CD4 Brilliant Violet 510™ | OKT4 |
| | 317429 | CD4 Pacific Blue | OKT4 |
| | 303504 | CD38 FITC | HIT2 |
| | 302326 | CD20 PerCP-Cy5.5 | 2H7 |
| | 311118 | CD24 APC | ML5 |
| | 350109 | CD294 (CRTH2) APC | BM16 |
| | 348224 | IgD Pacific Blue | IA6-2 |
| **BD Biosciences** | 557831 | CD14 APC-Cy7 | MϕP9 |
| **(San Diego, CA.** | 555547 | $TCR_{\alpha\beta}$ FITC | T10B9.1A-31 |
| **USA)** | 563071 | CCR3 Horizon™ BV510 | 5E8 |
| | 560199 | CD43 PE | 1G10 |
| | 561159 | CD5 Alexa Fluor® 700 | UCHT2 |
| | 560609 | CD27 Pe-Cy7 | M-T271 |
| | 551773 | CCR6 PE | 11A9 (RUO) |
| **eBiosciences** | 12-4776-42 | Fox P3 PE | PCH101 |
| **(San Diego, CA.** | 48-5699-42 | Ki67 eFluor® 450 | 20Raj1 |
| **USA)** | | | |

**Supplemental Acknowledgments**

AMS04 Study Site Investigators

Mark Agius, MD, Neurology, University of California at Davis, Sacramento, CA 95817

Michelle Apperson, MD, Neurology, University of California at Davis, Sacramento, CA 95817

James Bowen, MD, Multiple Sclerosis Center, Swedish Medical Center Foundation, Seattle, WA 98122

Margaret Burnett, MD, Neurology, University of Southern California, Los Angeles, CA 90033

Jonathan Calkwood, MD, Minneapolis Clinic of Neurology, MN 55422

Ann Camac, MD, Neurology, Lahey Clinic, Lexington, MA, 02421

Mirela Cerghet, MD, Neurology department, Henry Ford Health System, Detroit, MI 48202

Stanley Cohan, MD, PhD, Providence Multiple Sclerosis Center, Providence Brain and Spine Institute, Providence Health & Services, Portland, OR, 97225

Jill Conway, MD, Neurosciences Institute Neurology, Carolinas Medical Center, Charlotte, NC, 28207

Joanna Cooper, MD, Jordan Research & Education Institute, Berkeley, CA, 94705

John Corboy, MD, Neurology department, University of Colorado School of Medicine, University of Colorado, Denver, CO 80309

Corey Ford, MD, Neurology, University of New Mexico Health Sciences Center, Albuquerque, NM 87131